Dysregulated miR-34a-SIRT1-acetyl-p65 axis induces immune activation in chronic SIV-infection

Mahesh Mohan, Andrew A Lackner, Xavier Alvarez

Division of Comparative Pathology, Tulane National Primate Research Center

Tulane University Health Sciences Center, Covington, Louisiana- 70433

Introduction

1. The Gastrointestinal tract is a major target of HIV/SIV infection.

2. GI complications such as anorexia, weight loss and diarrhea are frequent and even reported in patients treated with anti-retroviral therapy.

3. An emerging feature of HIV/SIV pathogenesis is elevated levels of microbial translocation (Mbt) proposed to drive systemic immune activation/inflammation and disease progression.

4. Persistent GI inflammation is a hallmark of HIV/SIV infection and when not properly regulated can promote Mbt and systemic immune activation.

5. In addition to proinflammatory cytokines, transcription factors and chromatin modifiers, recent studies have proposed critical roles for miRNAs in controlling and managing certain aspects of the inflammatory process.

6. To identify and determine the immunoregulatory role of miRNAs, we profiled miRNA expression in the colon of chronically SIV-infected macaques.

Experimental Design

Intact colon specimens collected at necropsy

Chronic SIV-infected (N=12) (145-425 days PI)

Normal Uninfected Healthy Controls (N=4)

TaqMan Low Density Array (TLDA) Card A and B- 768 human miRNAs

Techniques Used:
TLDA, TaqMan stem loop and SYBR green qRT-PCR, Dual-luciferase reporter assay, Immunofluorescence and In situ hybridization

Data Analysis:
DataAssist v3.01
Multiple Comparison Corrections- Benjamini Hochberg method for false discovery rate
qRT-PCR- Non-parametric Wilcoxon's rank sum test
Luciferase Assay- unpaired "t" test

Results

miRNA ID	Acute SIV (n=12)										Uninfected Controls (n=4)				Fold Change	Adjusted *p* value
	HR11	HR48	GK31	GA19	G025	FT11	DV42	CP47	H36B	FE13	HG45	HG58	TL66	E307B	E188B	FK25		
hsa-miR-181a-2*	24.69	23.93	24.36	24.71	24.12	24.72	24.98	25.64	25.62	24.53	24.18	24.98	23.91	23.99	23.72	24.73	-1.5	0.0027
hsa-miR-628-5p	25.93	25.64	25.48	25.51	24.78	24.97	25.08	25.09	25.21	24.99	24.17	25.18	24.19	24.37	24.52	25.18	-1.6	0.0027
hsa-miR-378	25.83	24.87	25.34	25.27	24.63	25.78	25.27	25.76	26.15	24.71	25.87	25.46	24.93	24.87	24.95	25.83	-1.2	0.0174
hsa-miR-424	25.82	25.16	25.54	25.32	25.13	25.27	25.87	25.92	26.32	25.18	26.89	25.92	26.87	26.86	25.84	26.84	1.4	0.0174
hsa-miR-425*	25.22	24.29	24.98	25.06	25.15	25.41	25.44	25.38	25.91	24.68	24.96	25.13	24.44	24.57	24.24	24.97	-1.5	0.0174
hsa-miR-454*	29.52	28.61	29.69	29.78	29.31	29.79	29.77	29.31	29.51	29.23	29.63	29.39	28.23	28.68	28.42	28.87	-1.8	0.0174
hsa-miR-223*	25.99	24.89	25.66	25.48	25.57	24.65	25.35	26.13	26.65	26.33	26.53	26.75	26.54	27.23	26.67	28.97	2.7	0.019
hsa-miR-24-2*	25.36	24.79	25.31	24.98	25.64	24.75	24.92	25.58	25.33	24.98	24.65	25.22	24.51	24.78	24.48	25.18	-1.3	0.019
hsa-miR-520c-3p	32.61	29.79	32.98	31.39	31.86	31.12	31.94	32.16	31.29	31.80	31.51	31.28	30.51	30.63	30.31	31.39	-1.8	0.019
hsa-miR-34a	21.44	20.92	20.74	20.39	19.43	19.67	20.32	21.32	21.14	20.82	19.96	21.01	21.76	21.97	20.97	22.16	2.2	0.0306
hsa-miR-34a*	24.17	23.48	23.32	22.79	22.21	23.14	23.98	24.83	24.38	24.37	23.53	24.67	24.99	25.56	24.68	25.10	2.8	0.0315
hsa-let-7b	18.06	17.44	17.62	17.68	17.86	17.77	17.98	18.08	18.31	17.24	17.51	17.87	17.98	18.21	17.72	18.68	1.3	0.0278
hsa-miR-1930*	27.83	26.74	26.67	26.42	25.97	26.56	27.79	28.64	28.21	28.88	26.18	28.62	27.88	28.45	28.01	29.83	2.3	0.0589
hsa-miR-1468-5p	16.11	15.98	16.81	15.35	15.29	14.79	15.72	16.44	16.67	16.28	16.47	16.59	17.21	17.85	16.23	18.16	2.1	0.0719
hsa-miR-362	19.65	20.23	20.79	20.38	20.88	20.48	20.49	21.62	20.73	19.84	19.85	20.76	19.73	19.98	19.86	20.68	-1.3	0.0758
hsa-miR-744*	26.22	25.74	25.97	26.25	25.91	27.28	26.71	26.78	27.15	25.89	25.96	26.54	25.72	25.56	25.53	26.51	-1.5	0.0796
hsa-miR-18a	20.89	20.28	20.64	20.25	20.09	20.63	21.24	20.44	20.79	21.85	21.14	21.09	20.87	21.18	20.79	21.97	1.4	0.0821
hsa-miR-21	15.76	15.79	16.65	14.98	14.68	14.42	15.67	15.65	15.93	15.35	15.68	16.25	15.91	15.98	15.78	16.66	1.6	0.0821
hsa-miR-423a	24.87	24.61	24.74	24.78	24.63	24.38	25.17	24.44	24.92	25.44	23.89	25.08	25.45	25.23	25.88	24.68	-1.8	0.0821
hsa-miR-656	26.98	25.27	26.87	26.86	26.39	25.95	25.89	25.98	26.35	25.82	25.63	25.58	24.64	24.96	24.64	26.82	-1.9	0.0831
hsa-miR-22*	23.88	23.78	23.48	23.33	23.87	22.48	23.64	23.54	23.13	23.15	22.37	23.33	23.32	23.39	23.42	24.13	1.4	0.0841
hsa-miR-30c	15.71	14.74	14.86	14.83	14.53	14.76	14.88	15.15	15.17	14.48	14.53	14.92	14.51	14.55	14.17	15.17	-1.3	0.0847
hsa-miR-129-3p	26.83	26.55	25.28	25.31	26.12	25.96	26.87	25.54	26.79	24.73	24.34	24.95	24.48	25.00	24.19	25.34	-1.7	0.095

Table 1. Changes in miRNA expression in colon during chronic SIV infection. (**A**) The table shows raw CT and fold change for all differentially expressed (Adjusted p<0.05) miRNAs after applying multiple comparisons correction (Benjamini-Hochberg adjusted p values for false discovery rate) in the colon of rhesus macaques during chronic SIV infection.

Key Findings (Table 1 and Figure 1)

1. 10 miRNAs (3 up and 7 down) showed statistically significant differential expression. (Table 1). At least, 13 miRNAs showed a tendency for statistical significance (p<0.1).

2. We further characterized miR-34a, miR-21 and let-7b separately in colonic epithelium and LPL to determine their role in maintaining GI structure and function (Fig 1).

3. miR-34a expression was significantly elevated in both colonic epithelium and LPL (Fig 1A&D).

4. miR-21 and let-7b expression was significantly increased only in colonic epithelium (Fig 1B&C).

5. Since miR-34a and miR-21 are DNA damage responsive miRNAs we next determined if DNA damage response (DDR) signaling was activated in colonic epithelial and LPL compartments.

6. Accordingly, we performed immunofluorescence studies to determine the expression of the DDR protein marker γH2A.X in the colon.

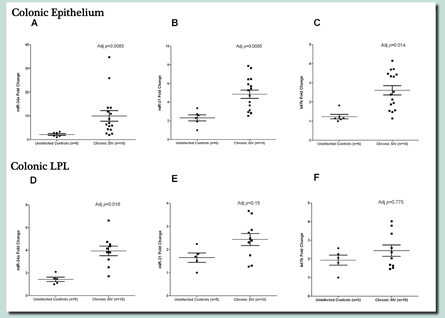


Figure 1. miR-34a, miR-21 and let-7b expression is significantly elevated in colon during chronic SIV infection. Panels **A-C** represent colonic epithelium and panels **D-F** represent colonic lamina propria leukocytes (LPLs). Note that while all 3 miRNAs showed enhanced expression in the epithelium (**A-C**), only miR-34a was statistically significantly elevated in both colonic epithelium and LPL compartments (**A&D**). Data was analyzed using non-parametric (wilcoxon's rank sum test) method and multiple comparisons correction was performed using Benjamini-Hochberg method (Adjusted *p* values shown for each panel). The error bars represent standard error of mean fold change within each group.

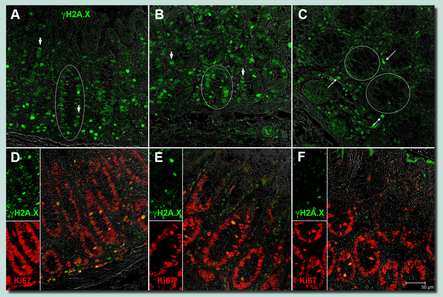


Figure 2. Colonic epithelial cells of chronic SIV-infected macaques strongly express the DNA damage response (DDR) sensor protein γH2A.X. (**A-B**). White circles in panels **A** and **B** demarcate the periphery of a crypt containing several γH2A.X. positive nuclei. Arrow heads (**A-B**) point to γH2A.X. positive crypt epithelial nuclei. In contrast, colonic epithelial cells from the normal uninfected control macaque show extremely low to undetectable γH2A.X expression (**C**). White circles in panel **C** demarcate the periphery of two crypts that show extremely weak to no γH2A.X. expression in the nuclei. Long thin arrows (**C**) point to γH2A.X. positive LPL. Colonic epithelial cells from both SIV-infected and control macaques also stained positive for Ki67, a cell proliferation marker suggesting that these cells did not become senescent (**D-E**). Epithelial and LPL γH2A.X (**A-C**) positive staining cells are shown in **green** (Alexa fluor-488). Epithelial and LPL Ki67 (**D-E**) positive staining cells are shown in **red** (Alexa fluor-568). Panels (**D-F**) involve double labels with γH2A.X. (**green**) and Ki67 (**red**). The individual channels (**green** for γH2A.X., and **red** for Ki67) and grey for differential interference contrast (DIC) to reveal tissue architecture appear on the left with a larger merged image on the right. Colocalization of **green** (γH2A.X.) and **red** (Ki67) appear light yellow. All panels are shown at 40X magnification.

Key Findings (Figure 2)

1. γH2A.X expression in the crypt epithelial nuclei of SIV-infected macaques suggests activation of DDR signaling due to inflammation induced oxidative stress (Fig 2A-C).

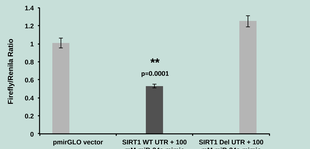
2. Since miR-34a and miR-21 are double stranded DNA damage responsive miRNAs, DDR as evidenced by increased gH2A.X expression could directly drive their elevated expression.

3. Increased expression of γH2A.X is also an initiating signal for cellular senescence.

4. Presence of Ki67 expression in majority of crypt epithelial cells suggests absence of cellular senescence (Fig 2D-F).

5. Nevertheless, chronic unresolved inflammation due to low-level viral replication reported in ART treated HIV patients can in due course cause cellular senescence leading to epithelial barrier dysfunction, microbial translocation and disease progression.

miR-34a can bind to the Rhesus macaque SIRT1 3' UTR and negatively regulate its expression



SIRT1 mRNA expression is signficantly reduced in colonic epithelium and LPL of chroncially SIV infected rhesus macaques

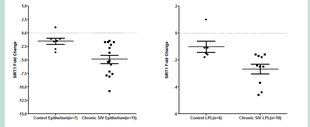


Figure 3. SIRT1 mRNA expression is significantly decreased in both colonic epithelium ($p=0.0118$) (**A**) and LPL ($p=0.015$) (**B**) compartments of chronic SIV-infected macaques. Data was analyzed using non-parametric (Wilcoxon's rank sum test for independent samples) method. The error bars represent standard error of mean fold change within each group. miR-34a physically associates with the 3' UTR of rhesus macaque SIRT1 mRNA ($p=0.0001$) (**C**). The SIRT1 wild type and deleted 3 ' UTR sequences were inserted into the multiple cloning sites situated in the 3' end of firefly luciferase gene in the pmirGLO vector. HEK293 cells were co-transfected with 100 nM miR-34a mimic and 100 ng of luciferase reporter constructs containing wild type or deleted SIRT1 3'UTR sequences. Firefly and *Renilla* luciferase activities were detected using the Dual-Glo luciferase assay system 48 h after transfection. The ratio of luciferase activities (Firefly/*Renilla*) was calculated and normalized to the wells transfected with only unmanipulated pmir-GLO vector.

Summary (Table 1 and Figures 1-3)

1. Chronic SIV infection is characterized by elevated prosenescent miR-34a and reduced anti-senescent SIRT1 expression in the colonic epithelium of chronically SIV-infected macaques.

2. Enhanced miR-34a and reduced SIRT1 expression was also detected in the colonic lamina propria leukocyte (LPL) compartment.

3. As the LPL compartment is enriched for immune cells and primarily involved in mediating immune/inflammatory responses we focused on the RelA/p65 subunit of NFκB, a transcription factor central to immune and inflammatory responses.

4. Most notably, post-translational modifications such as phosphorylation, acetylation, sumoylation, etc. are necessary for modulating NFκB mediated gene expression.

5. Among these, acetylation of lysine 310 is crucial for full activation of NFκB transcriptional potential.

6. More importantly, SIRT1 and HDAC3 can deacetylate lysine 310 on p65 thereby inhibiting its transcriptional activity.

7. Consequently, we performed immunofluorescence studies to determine if miR-34a mediated SIRT1 downregulation resulted in elevated expression of acetylated p65 (lysine 310).

Large numbers of acetylated p65 positive cells are detectable in the LPL compartment of chronic SIV-infected macaques (A, B, C) and not in uninfected control macaques (D, E, F).

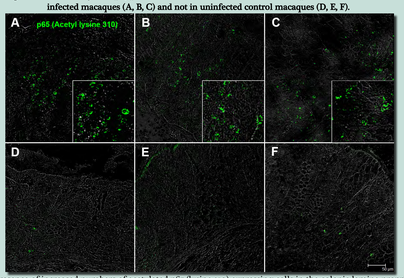


Figure 4. Presence of increased numbers of acetylated p65 (lysine 310) expressing cells in the colonic lamina propria of three chronic-SIV infected rhesus macaques (**A-C**). The inset image shows a close-up magnified view of acetylated p65 positive cells in the colonic lamina propria. Note the fewer acetylated p65 (lysine 310) positive cells in the three uninfected control macaques (**D-F**). Acetylated p65 (lysine 310) positive staining cells are shown in green (Alexa fluor-488). All panels are shown at 40X magnification.

Lymphocytes (A) and Macrophages (B and C) are NOT the immune cell types in the LPL compartment of chronic SIV-infected macaques that co-express acetylated p65.

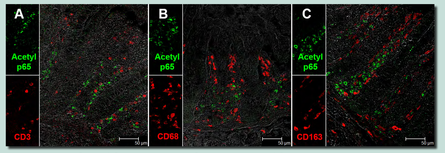


Figure 5. Lymphocytes [CD3 (**A**)] and macrophages [CD68 (**B**), CD163 (**C**)] are not the predominant cellular source of acetylated p65 (lysine 310). All panels involve double labels with acetylated p65 in **green** and CD_3 for lymphocytes and CD68/CD163 for macrophages in **red**. For each panel the individual channels (**green** for acetylated p65, and **red** for CD_3, CD68 and CD163) and grey for differential interference contrast (DIC) to reveal tissue architecture appear on the left with a larger merged image on the right. Note that acetylated $p65^+$ cells do not colocalize with CD_3, CD68 and CD163. All panels are 40X magnification.

Significant numbers of IgA secreting plasma cells (A, B and C) in the LPL compartment of chronic SIV-infected macaques are the predominant source of acetylated p65 (lysine 310).

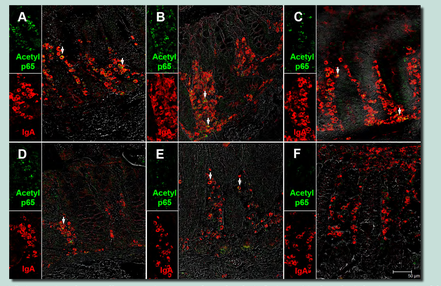


Figure 6. IgA secreting plasma cells are a major source of acetylated p65 (lysine 310) in the colonic lamina propria of three chronic-SIV infected rhesus macaques (**A-C**). All panels involve double labels with acetylated p65 (**green**) and IgA (**red**) for plasma cells. For each panel the individual channels (**green** for acetylated p65, and **red** for IgA and grey for differential interference contrast (DIC) to reveal tissue architecture appear on the left with a larger merged image on the right. Colocalization of **green** (acetylated p65) and **red** (IgA) appear light yellow and is indicated by white arrow heads. Note the fewer IgA^+ and IgA/Acetyl $p65^+$ plasma cells in the three uninfected control macaques (**D-F**). All panels are shown at 40X magnification.

Significant numbers of IgG secreting plasma cells (A, B and C) in the LPL compartment of chronic SIV-infected macaques also co-express acetylated p65 (lysine 310).

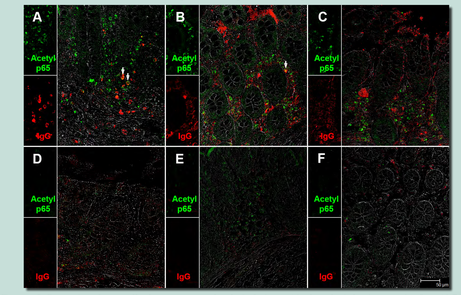


Figure 7. IgG secreting plasma cells also express acetylated p65 (lysine 310) in the colonic lamina propria of two (**A-B**) out of three chronic-SIV infected rhesus macaques (**A-C**). All panels involve double labels with acetylated p65 (**green**) and IgG (**red**) for plasma cells. For each panel the individual channels (**green** for acetylated p65, and **red** for IgG and grey for differential interference contrast (DIC) to reveal tissue architecture appear on the left with a larger merged image on the right. Colocalization of green (acetylated p65) and red (IgG) appear light yellow and is indicated by white arrow heads. Note the paucity of IgG/acetyl $p65^+$ plasma cells in the uninfected control macaques (**D-F**). All panels are shown at 40X magnification.

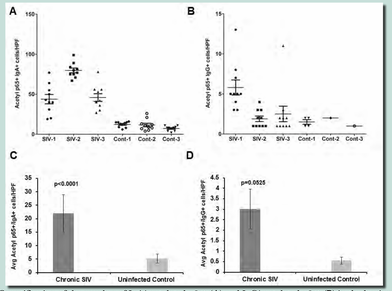


Figure 8. Quantification of the number of IgA/acetylated $p65^+$ (**A**) and IgG/acetylated $p65^+$ (**B**) in the lamina propria of 3 chronic SIV-infected and 3 control rhesus macaques. Positive cells were counted at an original magnification of 40X in a total of 10 high power fields (HPF). One HPF= 0.2827 mm^2. Each data point represents the number of cells in a single HPF; the error bars represent the mean values. Average IgA/acetylated $p65^+$ (**C**) and IgG/acetylated $p65^+$ (**D**) in the colonic lamina propria of 3 SIV-infected and 3 uninfected control macaques. Data was analyzed using wilcoxon's rank sum test.

miR-34a localizes to the colonic epithelium and IgA secreting plasma cells in the LPL compartment of chronic SIV-infected macaques (A and B). Intense expression of miR-34a in the colonic epithelium and LPL compartment confirms qRT-PCR data shown in figure 2A&D.

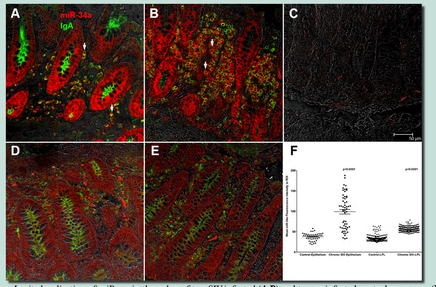


Figure 9. *In situ* localization of miR-34a in the colon of two SIV-infected (**A-B**) and two uninfected control macaques (**D-E**) with wild type miR-34a or scrambled probe (**C**). All panels involve double labels with miR-34a (**red**) and IgA (**green**) for plasma cells. The grey channel represents differential interference contrast (DIC) to reveal tissue architecture. Colocalization of **green** (IgA) and **red** (miR-34a) appear light yellow. Note the intense miR-34a staining in the epithelium and markedly increased numbers of $IgA^+miR\text{-}34a^+$ plasma cells (white arrow heads) in the colon of the SIV-infected macaques (**A-B**). In contrast, miR-34a staining is weak in the colonic epithelium and LPL of the control macaques (**D-E**). The scrambled probe did not yield a signal (**C**). All panels are 40X magnification. Quantification of cells and regions of interest (ROI) labeled by LNA-modified miR-34a probe was performed using Volocity 5.5 software after capturing images on a Leica confocal microscope. Several ROI were hand drawn on the epithelial and LPL regions in the images from colon (**F**). Image analysis data was analyzed using wilcoxon's rank sum test.

Summary (Figures 3-9) and Conclusions

1. Plasma cell numbers that increase substantially in chronically inflamed tissues can activate the NFκB pathway in response to proinflammatory factors.

2. Presence of NFκB binding/response elements on the miR-34a promoter suggests a direct NFκB mediated mechanism in driving increased miR-34a expression.

3. miR-34a can then directly bind to the SIRT1 3' UTR and downregulate its expression.

4. SIRT1 deacetylates lysine 310 residue on p65. Reduced SIRT1 expression can maintain p65 in its transcriptionally active form and in this way generate a feed forward mechanism involving NFκB, miR-34a and SIRT1 leading to constitutive activation and transcription of NFκB responsive genes.

5. IgG producing long-lived plasma cells in the colonic lamina propria of IBD patients produce MMP-3, a NFκB responsive matrix metalloproteinase linked to tissue destruction.

6. IgG plasma cells in the colonic mucosa of IBD patients can also induce TNF-κand IL-1β production by $CD14^+$ macrophages via IgG-IC-FcγR signaling thereby aggravating colonic inflammation.

7. Overall, intestinal plasma cells may have broader functions in modulating inflammatory responses that can directly contribute to epithelial barrier disruption and miR-34a-SIRT1-mediated constitutive NFκB activation may assist in these functions.

Supported by NIH grants: R01DK089929 to MM, AI084793 and OD011104 (formerly RR00164)

©Copyright 2014, TNPRC Media Lab
Tulane University